Intracellular, extracellular, and membrane forces in remodeling and mechanotransduction: The mechanical bidomain model

Article · September 2015

DOI: 10.1166/jcsmd.2015.1079

CITATIONS
3

READS
129

4 authors:

Kharananda Sharma
Oakland University
6 PUBLICATIONS **22** CITATIONS
SEE PROFILE

Nofe Al-Asuoad
Oakland University
5 PUBLICATIONS **7** CITATIONS
SEE PROFILE

Meir Shillor
Oakland University
211 PUBLICATIONS **3,680** CITATIONS
SEE PROFILE

Bradley J Roth
Oakland University
309 PUBLICATIONS **7,814** CITATIONS
SEE PROFILE

Journal of Coupled Systems and Multiscale Dynamics

doi:10.1166/jcsmd.2015.1079
J. Coupled Syst. Multiscale Dyn.
Vol. 3(3)/2330-152X/2015/200/008

Research Article

Intracellular, extracellular, and membrane forces in remodeling and mechanotransduction: The mechanical bidomain model

Kharananda Sharma[1], Nofe Al-Asuoad[2], Meir Shillor[2], and Bradley J. Roth[1,*]

[1]*Department of Physics, Oakland University, Rochester, MI 48309, United States*
[2]*Department of Mathematics and Statistics, Oakland University, Rochester, MI, 48309, United States*

(Received: 10 February 2015. Accepted: 28 April 2015)

ABSTRACT

In the mechanical bidomain model, cardiac tissue is represented by a macroscopic model that accounts for the microscopic coupling between the extracellular matrix, the cytoskeleton, and integrin proteins in the membrane. We develop this model by considering intracellular and extracellular displacements, **u** and **w**, individually. The central hypothesis of the model is that the difference **u** − **w** is responsible for the membrane force. In this paper, analytical solutions are provided for two simple problems in biomechanics: a tissue subject to a shear force and a tissue subject to a pressure force. An implementation of the model using finite elements allows the numerical simulation of biomechanics problems. The importance of the mechanical bidomain model lies in its multiscale structure in the form of two coupled systems. This model can be used to study crucial physiological events such as mechanotransduction and tissue remodeling.

Keywords: Biomechanics, Finite Element, Mechanical Bidomain Model, Mechanotransduction, Remodeling, Stress.
Section: Mathematical, Physical & Engineering Sciences

1. INTRODUCTION

Mechanotransduction is the process by which tissue converts a mechanical signal to a biological response. For example, vascular endothelium responds to mechanical signals from blood flow by regulating vasodilation or vasoconstriction, or by increasing the production of growth factors.[1] Another example is when mechanical interactions between ischemic and nonischemic regions of the heart trigger remodeling of cardiac tissue.[2] What is the mechanism underlying the detection of these mechanical signals?

Past studies suggest that the underlying cause of mechanotransduction is tissue stress or strain.[3–8] Other research, however, indicates that the response of tissue to mechanical signals is modulated by membrane proteins, such as integrins.[9–14] If integrins are critical to mechanotransduction, then the important mechanical quantity is not the tissue stress or strain, but rather forces acting on the integrins across the cell membrane. To predict where and when mechanotransduction occurs, we need a mathematical model that focuses on membrane forces rather than stresses and strains in the intracellular and extracellular space.

Over the last four years, we have developed a way to predict where membrane forces are large: the *mechanical bidomain model*.[15–23] In Figure 1, the mechanical properties of the extracellular space are represented by an array of springs (blue), as are the properties of the intracellular space (green). The membrane is accounted for by an array

*Author to whom correspondence should be addressed.
Email: roth@oakland.edu

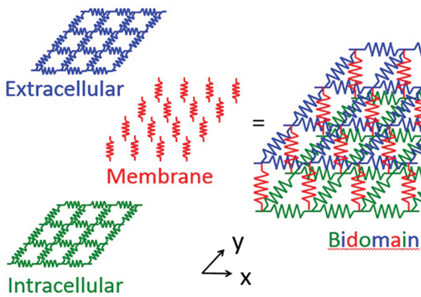

Fig. 1. A schematic diagram of the mechanical bidomain model. The elastic properties of the intracellular space are depicted by the green grid of springs, and the properties of the extracellular space by the blue grid. The two spaces are coupled by the membrane, shown as an array of red springs. This is a two-dimensional model, so stretching of the membrane springs is not caused by the displacements in the z direction perpendicular to the sheet. Rather, if the intra- and extracellular spaces are displaced by different amounts in the $x-y$ plane, the membrane springs stretch causing membrane forces.

of springs (red) coupling the two spaces. The fundamental hypothesis of this model is that mechanotransduction is caused by the stretching of the membrane springs, and not the stresses and strains in the intracellular or extracellular spaces.

To illustrate the importance of the bidomain model, consider Figures 2 and 3. In Figure 2 the strain in the intra- and extracellular spaces is zero. The blue and green grids of springs look the same as in Figure 1. But, if the extracellular space is displaced uniformly to the left relative to the intracellular space, the red membrane springs are all stretched and integrins experience forces throughout the tissue, causing mechanotransduction. On the other hand, in Figure 3 the intra- and extracellular spaces undergo a complicated, heterogeneous strain. Some springs are stretched and others are compressed. But, if the strain is identical in the two spaces, none of the red membrane springs are stretched, integrins do not experience forces anywhere, and there is no mechanotransduction.

Figures 1–3 summarize a new conceptual framework for mechanotransduction. These figures are visualizations that illustrate key predictions of the mathematical model. The model changes the way we view biomechanics. Biomechanical models have existed for decades, but they often do

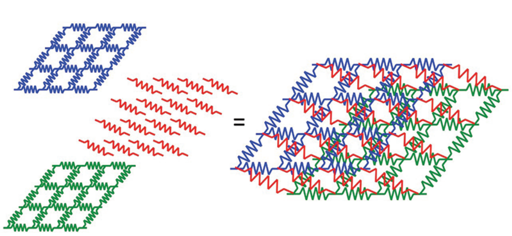

Fig. 2. The intra- and extracellular spaces are unstrained, but the extracellular space is displaced relative to the intracellular space. The membrane springs are all stretched.

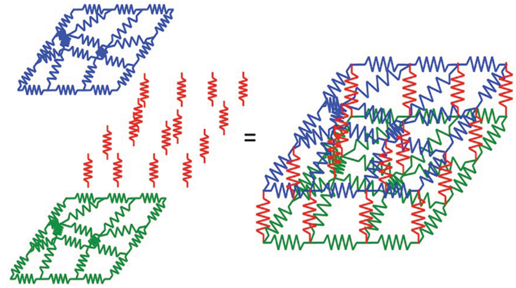

Fig. 3. The intra- and extracellular spaces are strained in a complicated and heterogeneous way, but the strains are identical in the two spaces. The membrane springs are not stretched.

not predict the distribution of membrane forces throughout the tissue because they are not "bidomain" models (models that treat the intra- and extracellular spaces *separately*, coupled by the membrane). Our model challenges the existing paradigm of "monodomain" models (models that do *not* separate the intra- and extracellular spaces).

The hypothesis that membrane forces are responsible for mechanotransduction has been suggested qualitatively by many researchers (for example, Refs. [9, 24–27]). Indeed, studies using a single layer of cells on an extracellular substrate have adopted this framework, referring to the membrane forces as the *traction force*.[28, 29] Our goal is to incorporate these ideas into a mathematical model, and to make quantitative predictions about membrane or traction forces. Important processes such as remodeling around an ischemic region in the heart or the mechanical response of blood vessels depend crucially on the underlying concept of the mechanism for mechanotransduction.

2. METHODS

The *microscopic* response to mechanical forces is important for understanding the biomechanics of molecules and cells. It is equally important, however, to understand the *macroscopic* biomechanical properties of tissue. Most macroscopic models do not study the behavior of the intracellular and the extracellular spaces separately. In the mechanical bidomain model, cardiac tissue is represented by a macroscopic model that accounts for the microscopic coupling between the extracellular matrix, the cytoskeleton, and integrin proteins.

We represent tissue as a two-phase material with intracellular and extracellular spaces. These spaces are linked by the membrane. The intracellular and extracellular displacements are denoted by $\mathbf{u}$ and $\mathbf{w}$. The difference in the displacement between the two spaces, $\mathbf{u}-\mathbf{w}$, gives rise to mechanical forces in the cell membrane. We use stress–strain relationships to derive the equations of the mechanical bidomain model. The intracellular stress and strain are related by

$$\tau_{ixx} = -p + 2\nu\epsilon_{ixx} + \gamma\epsilon_{ixx} + T \quad (1)$$

$$\tau_{iyy} = -p + 2\nu\epsilon_{iyy} \tag{2}$$

$$\tau_{ixy} = 2\nu\epsilon_{ixy} \tag{3}$$

and the extracellular stress and strain are related by

$$\tau_{exx} = -q + 2\mu\epsilon_{exx} \tag{4}$$

$$\tau_{eyy} = -q + 2\mu\epsilon_{eyy} \tag{5}$$

$$\tau_{exy} = 2\mu\epsilon_{exy} \tag{6}$$

where τ_{ixx} and τ_{exx} are normal intra- and extracellular stresses in the x direction, τ_{iyy} and τ_{eyy} are normal intra- and extracellular stresses in the y direction, and τ_{ixy} and τ_{exy} are the intra- and extracellular shear stresses. ϵ_{ixx} and ϵ_{exx} are intra- and extracellular strains in the x direction, ϵ_{iyy} and ϵ_{eyy} are intra- and extracellular strains in the y direction, and ϵ_{ixy} and ϵ_{exy} are intra- and extracellular shear strains. The parameter γ is the Young's modulus along the myocardial fibers, and ν and μ are the shear moduli of the intra- and extracellular spaces. The quantities p and q are intra- and extracellular hydrostatic pressures, and T is an active tension along the fibers, which are assumed to be aligned with the x-axis.

In two-dimensional Cartesian coordinates, we can express the linearized strain components in terms of $\mathbf{u}$ and $\mathbf{w}$ by

$$\epsilon_{ixx} = \frac{\partial u_x}{\partial x} \tag{7}$$

$$\epsilon_{iyy} = \frac{\partial u_y}{\partial y} \tag{8}$$

$$\epsilon_{ixy} = \frac{1}{2}\left(\frac{\partial u_x}{\partial y} + \frac{\partial u_y}{\partial x}\right) \tag{9}$$

$$\epsilon_{exx} = \frac{\partial w_x}{\partial x} \tag{10}$$

$$\epsilon_{eyy} = \frac{\partial w_y}{\partial y} \tag{11}$$

$$\epsilon_{exy} = \frac{1}{2}\left(\frac{\partial w_x}{\partial y} + \frac{\partial w_y}{\partial x}\right). \tag{12}$$

Biological tissue is mainly composed of water; therefore, the intra- and extracellular spaces are each incompressible, $\partial u_x/\partial x + \partial u_y/\partial y = 0$ and $\partial w_x/\partial x + \partial w_y/\partial y = 0$. The equations of mechanical equilibrium are

$$\frac{\partial \tau_{ixx}}{\partial x} + \frac{\partial \tau_{ixy}}{\partial y} = K(u_x - w_x) \tag{13}$$

$$\frac{\partial \tau_{exx}}{\partial x} + \frac{\partial \tau_{exy}}{\partial y} = -K(u_x - w_x) \tag{14}$$

$$\frac{\partial \tau_{ixy}}{\partial x} + \frac{\partial \tau_{iyy}}{\partial y} = K(u_y - w_y) \tag{15}$$

$$\frac{\partial \tau_{exy}}{\partial x} + \frac{\partial \tau_{eyy}}{\partial y} = -K(u_y - w_y). \tag{16}$$

The parameter K is the spring constant coupling the intra- and extracellular spaces, and is a new parameter unique to the bidomain model. We have little experimental knowledge about K. We assume this spring constant is uniform, Hookean (K is independent of stretch), temperature independent, and isotropic. This represents the simplest assumption about the intracellular-extracellular coupling; more realistic assumptions may be needed to fit experimental data more accurately.

Upon substituting (1)–(12) into (13)–(16), we get the mechanical bidomain equations in terms of displacements and pressures together with the two incompressibility equations

$$-\frac{\partial p}{\partial x} + (2\nu+\gamma)\frac{\partial^2 u_x}{\partial x^2} + \nu\frac{\partial^2 u_x}{\partial y^2} + \nu\frac{\partial^2 u_y}{\partial y \partial x} + \frac{\partial T}{\partial x} = K(u_x - w_x) \tag{17}$$

$$-\frac{\partial q}{\partial x} + 2\mu\frac{\partial^2 w_x}{\partial x^2} + \mu\frac{\partial^2 w_x}{\partial y^2} + \mu\frac{\partial^2 w_y}{\partial y \partial x} = -K(u_x - w_x) \tag{18}$$

$$-\frac{\partial p}{\partial y} + 2\nu\frac{\partial^2 u_y}{\partial y^2} + \nu\frac{\partial^2 u_y}{\partial x^2} + \nu\frac{\partial^2 u_x}{\partial x \partial y} = K(u_y - w_y) \tag{19}$$

$$-\frac{\partial q}{\partial y} + 2\mu\frac{\partial^2 w_y}{\partial y^2} + \mu\frac{\partial^2 w_y}{\partial x^2} + \mu\frac{\partial^2 w_x}{\partial x \partial y} = -K(u_y - w_y). \tag{20}$$

In the next section, we will examine two analytical solutions to the bidomain equations that highlight the tissue behavior. The first focuses on shear forces at the tissue boundary,[22] and the second explores the interpretation of the tissue pressure.[23]

3. RESULTS

3.1. A Slab of Tissue Subject to Shear

Consider a long slab of cardiac tissue having its width equal to $2L$, as shown in Figure 4.[22] The fibers lie along

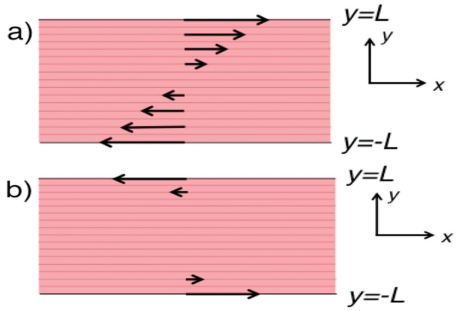

Fig. 4. A long, two-dimensional slab of cardiac tissue. The fibers (thin horizontal lines) lie along the x-axis. A shear force is applied to the extracellular space at the tissue boundary $y = \pm L$; the intracellular space is free at the boundary. (a) The intracellular and extracellular displacements, $\mathbf{u}$ and $\mathbf{w}$, as functions of y. The value of the length constant σ is small enough so that the difference between $\mathbf{u}$ and $\mathbf{w}$ is negligible on this scale. (b) The difference between the extracellular displacement and the intracellular displacement, $\mathbf{u} - \mathbf{w}$. The length of the arrows is magnified compared to panel a). The difference $\mathbf{u} - \mathbf{w}$ is significant only within a few length constants of the tissue surface.

the x-axis. At the tissue boundary, the intracellular space is stress free but a shear force F is applied in the extracellular space, directed to the right on the top boundary and to the left on the bottom. Assuming that the tissue has infinite length, we find from symmetry conditions that the displacements depend on only the y-coordinate. A solution of (17)–(20) is

$$u_x = Ay + B\sinh\left(\frac{y}{\sigma}\right), \quad u_y = 0, \quad p = 0 \tag{21}$$

$$w_x = Cy + D\sinh\left(\frac{y}{\sigma}\right), \quad w_y = 0, \quad q = 0 \tag{22}$$

where A, B, C, D and σ are parameters to be determined. The solution must satisfy the equilibrium equations. Plugging (21)–(22) into (17)–(20) gives

$$\nu\frac{B}{\sigma^2}\sinh\left(\frac{y}{\sigma}\right) = K\left(Ay + B\sinh\left(\frac{y}{\sigma}\right) - Cy - D\sinh\left(\frac{y}{\sigma}\right)\right) \tag{23}$$

$$\mu\frac{D}{\sigma^2}\sinh\left(\frac{y}{\sigma}\right) = -K\left(Ay + B\sinh\left(\frac{y}{\sigma}\right) - Cy - D\sinh\left(\frac{y}{\sigma}\right)\right). \tag{24}$$

Equations (23)–(24) are satisfied if

$$A = C \tag{25}$$

$$D = -\frac{\nu}{\mu}B \tag{26}$$

$$\sigma = \sqrt{\frac{\nu\mu}{K(\nu+\mu)}}. \tag{27}$$

To obtain the values of the unknown parameters B and C, we impose boundary conditions. At the surface of the tissue ($y = \pm L$), the normal stresses, τ_{iyy} and τ_{eyy}, are zero. The shear stresses are $\tau_{ixy} = 0$ and $\tau_{exy} = \pm F$. As a result of these boundary conditions, we get

$$A + \frac{B}{\sigma}\cosh\left(\frac{L}{\sigma}\right) = 0 \tag{28}$$

$$C + \frac{D}{\sigma}\cosh\left(\frac{L}{\sigma}\right) = \frac{F}{\mu}. \tag{29}$$

Solving (28)–(29) using (25)–(27), we get the displacements in terms of the applied shear force F as

$$u_x = \frac{F}{(\nu+\mu)}\left(y - \sigma\frac{\sinh(y/\sigma)}{\cosh(L/\sigma)}\right) \tag{30}$$

$$w_x = \frac{F}{(\nu+\mu)}\left(y + \frac{\nu}{\mu}\sigma\frac{\sinh(y/\sigma)}{\cosh(L/\sigma)}\right). \tag{31}$$

The first terms in both the intra- and extracellular displacements are identical. This common term predicts the monodomain behavior and does not contribute to the membrane force. The second terms, however, are different. These terms predict the bidomain behavior. Because the bidomain terms are different, they contribute to the membrane force. The difference in the horizontal displacements is

$$u_x - w_x = -\frac{F}{\mu}\sigma\frac{\sinh(y/\sigma)}{\cosh(L/\sigma)}. \tag{32}$$

The intracellular and extracellular shear strains are

$$\epsilon_{ixy} = \frac{F}{2(\nu+\mu)}\left(1 - \frac{\cosh(y/\sigma)}{\cosh(L/\sigma)}\right) \tag{33}$$

$$\epsilon_{exy} = \frac{F}{2(\nu+\mu)}\left(1 + \frac{\nu}{\mu}\frac{\cosh(y/\sigma)}{\cosh(L/\sigma)}\right). \tag{34}$$

The intracellular shear strain vanishes at the surface ($y = L$). The extracellular shear strain at the surface is $F/2\mu$.

The function $\cosh(y/\sigma)$ behaves like an exponential with length constant σ. Therefore, the membrane force is large over only a thin boundary layer near the tissue surface (Fig. 4(b)). However, the shear strains (33)–(34) are large throughout the tissue. This is a testable prediction of the bidomain model: if the strain is responsible for mechanotransduction the response will be distributed throughout the tissue, but if the membrane force is responsible for mechanotransduction the response will be localized near the tissue surface.

3.2. A Slab of Tissue Subject to Pressure

The slab shown in Figure 4, subject to a shear force at the surface, resulted in no intracellular or extracellular pressure ($p = q = 0$). If, on the other hand, we apply a normal force at the surface, we must examine the pressure in detail. In a previous publication, we found that to completely characterize the distributions of pressure we had to relax our assumption of incompressibility, and instead assume the intra- and extracellular spaces had bulk moduli χ and δ.[23] The pressure in each space is the negative of the product of the bulk modulus and the dilatation (the divergence of the displacement), in the limit as the bulk modulus goes to infinity and the dilatation goes to zero.

Consider an isotropic slab of tissue, like in the previous example, subject to a pressure P_0 at the surfaces $y = \pm L$. The strains can be related to the intra- and extracellular displacements, $\mathbf{u}$ and $\mathbf{w}$, by

$$\epsilon_{ixx} = 0, \quad \epsilon_{iyy} = \frac{\partial u_y}{\partial y}, \quad \epsilon_{ixy} = 0 \tag{35}$$

$$\epsilon_{exx} = 0, \quad \epsilon_{eyy} = \frac{\partial w_y}{\partial y}, \quad \epsilon_{exy} = 0. \tag{36}$$

The relationships between intracellular and extracellular stresses and strains are then

$$\tau_{iyy} = (\chi + 2\nu)\epsilon_{iyy} \tag{37}$$

$$\tau_{eyy} = (\delta + 2\mu)\epsilon_{eyy}. \tag{38}$$

The equations of mechanical equilibrium are

$$\frac{\partial \tau_{iyy}}{\partial y} = K(u_y - w_y) \tag{39}$$

$$\frac{\partial \tau_{eyy}}{\partial y} = -K(u_y - w_y). \tag{40}$$

Let

$$u_x = 0, \quad u_y = Ay + B\sinh\left(\frac{y}{\xi}\right) \tag{41}$$

$$w_x = 0, \quad w_y = Cy + D\sinh\left(\frac{y}{\xi}\right) \tag{42}$$

be solutions of the equations of the mechanical bidomain model. Plugging (41)–(42) into (35)–(40) and then solving, and assuming $\chi, \delta \gg \mu, \nu$, we find

$$A = C \tag{43}$$

$$D = -\frac{\chi}{\delta}B \tag{44}$$

$$\xi = \sqrt{\frac{\chi\delta}{K(\chi+\delta)}}. \tag{45}$$

We determine the values of B and C by applying the boundary conditions. At the surface of the tissue ($y = \pm L$), the boundary conditions are $\tau_{iyy} = 0$ and $\tau_{eyy} = \mp P_0$. The displacements that obey the equations of mechanical equilibrium and the boundary conditions are

$$u_y = -\frac{P_0}{(\chi+\delta)}\left(y - \xi\frac{\sinh(y/\xi)}{\cosh(L/\xi)}\right) \tag{46}$$

$$w_y = -\frac{P_0}{(\chi+\delta)}\left(y + \xi\frac{\chi}{\delta}\frac{\sinh(y/\xi)}{\cosh(L/\xi)}\right). \tag{47}$$

The difference in displacements, $u_y - w_y$ causes a membrane force

$$u_y - w_y = \frac{P_0\xi}{\delta}\frac{\sinh(y/\xi)}{\cosh(L/\xi)}. \tag{48}$$

The membrane force is largest near the boundary, $y = \pm L$. However, the displacements and the difference in displacements, $u_y - w_y$, go to zero as χ and δ go to infinity so that the membrane force vanishes for an incompressible tissue. The pressures $p = -\chi\epsilon_{iyy}$ and $q = -\delta\epsilon_{eyy}$ remain finite when χ and δ go to infinity (but χ/δ is finite)

$$p = \frac{\chi}{\chi+\delta}P_0\left(1 - \frac{\cosh(y/\xi)}{\cosh(L/\xi)}\right) \tag{49}$$

$$q = \frac{\delta}{\chi+\delta}P_0\left(1 + \frac{\chi}{\delta}\frac{\cosh(y/\xi)}{\cosh(L/\xi)}\right). \tag{50}$$

We can express the pressures as the sum of two terms, P and Q. The "monodomain" pressure is $P = p + q$ and the "bidomain" pressure is $Q = p - (\chi/\delta)q$.

The distribution of pressures P and Q are shown in Figure 5. This calculation leads to two important conclusions. First, in the limit as the bulk moduli go to infinity, the displacement and membrane force go to zero. Pressure should be relatively ineffective at producing mechanotransduction compared to shear. Second, the intra- and extracellular pressure distributions consist of a monodomain part (first terms in (49) and (50)) and a bidomain part (second terms). The bidomain part falls off with distance from the surface with length constant ξ. Thus, two new length constants arise from the mechanical bidomain model: σ, which depends on the shear moduli, and ξ which depends on the bulk moduli. Additional implications of relaxing the assumption of incompressibility can be found in Ref. [23].

3.3. Numerical Simulations Using the Finite Element Method

The analytical solutions in the previous two sections provide much insight into the behavior of the mechanical bidomain model. To solve more realistic and complex problems, however, we need to develop numerical methods. We have some preliminary computational simulations based on a finite difference method,[15, 16] but these techniques are limited to simple tissue shapes and fiber geometries. To take advantage of the full power of the model, we need to implement our calculations using the finite element method. In this section, we present our first results computed using finite elements. We examine the problem of a tissue slab subject to a shear force introduced in Section 3.1. The model, however, is general and can be applied to any tissue geometry.

Consider a two-dimensional, rectangular setting $D = [0, a] \times [-L, L]$, where the fibers are oriented in the x direction. Let $\partial D = \Gamma = \bar{\Gamma}_D \cup \bar{\Gamma}_N$ denote the boundary of D, as depicted in Figure 6. The model is based on the equations of Section 3.2 for compressible tissue. The intracellular stress tensor is

$$\tau_{ixx} = \chi(\epsilon_{ixx} + \epsilon_{iyy}) + 2\nu\epsilon_{ixx} \tag{51}$$

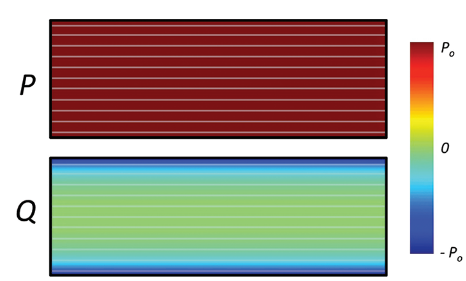

Fig. 5. A long two dimensional slab of cardiac tissue. The fibers (thin horizontal lines) lie along the x-axis. A pressure P_0 is applied to the extracellular space at the tissue boundary $y = \pm L$; the intracellular space is free at the boundary. (a) The monodomain pressure P, which is uniform throughout the tissue. (b) The bidomain pressure Q, which is significant only within a few length constants of the surface.

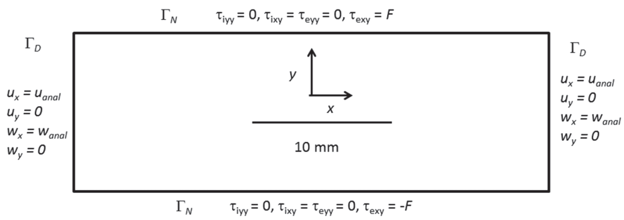

Fig. 6. 2-D slab of cardiac tissue.

$$\tau_{iyy} = \chi(\epsilon_{ixx} + \epsilon_{iyy}) + 2\nu\epsilon_{iyy} \quad (52)$$

$$\tau_{ixy} = 2\nu\epsilon_{ixy} \quad (53)$$

and the extracellular stress tensor is

$$\tau_{exx} = \delta(\epsilon_{exx} + \epsilon_{eyy}) + 2\mu\epsilon_{exx} \quad (54)$$

$$\tau_{eyy} = \delta(\epsilon_{exx} + \epsilon_{eyy}) + 2\mu\epsilon_{eyy} \quad (55)$$

$$\tau_{exy} = 2\mu\epsilon_{exy}. \quad (56)$$

In this case, the mechanical bidomain model can be written

$$(\chi + 2\nu)\frac{\partial^2 u_x}{\partial x^2} + \nu\frac{\partial^2 u_x}{\partial y^2} + (\chi + \nu)\frac{\partial^2 u_y}{\partial x \partial y} = K(u_x - w_x) \quad (57)$$

$$(\delta + 2\mu)\frac{\partial^2 w_x}{\partial x^2} + \mu\frac{\partial^2 w_x}{\partial y^2} + (\delta + \mu)\frac{\partial^2 w_y}{\partial x \partial y} = -K(u_x - w_x) \quad (58)$$

$$(\chi + 2\nu)\frac{\partial^2 u_y}{\partial y^2} + \nu\frac{\partial^2 u_y}{\partial x^2} + (\chi + \nu)\frac{\partial^2 u_x}{\partial x \partial y} = K(u_y - w_y) \quad (59)$$

$$(\delta + 2\mu)\frac{\partial^2 w_y}{\partial y^2} + \mu\frac{\partial^2 w_y}{\partial x^2} + (\delta + \mu)\frac{\partial^2 w_x}{\partial x \partial y} = -K(u_y - w_y). \quad (60)$$

These equations are the same as (17)–(20), except for the inclusion of the intra- and extracellular bulk moduli χ and δ, the intra- and extracellular pressures are replaced by $p = -\chi(\epsilon_{ixx} + \epsilon_{iyy})$ and $q = -\delta(\epsilon_{exx} + \epsilon_{eyy})$, and we set $\gamma = T = 0$ implying there is no active tension in the tissue.

The boundary conditions for the upper and lower surfaces (Γ_N, $y = \pm L$) are the same as in Section 3.1: $\tau_{iyy} = 0$, $\tau_{ixy} = 0$, $\tau_{eyy} = 0$, $\tau_{exy} = \pm F$. Our analytical solution modeled an infinitely long slab in the x direction. In the finite numerical slab, we used the analytical solutions u_{anal} and w_{anal} ((30) and (31)) for the boundary condition at the left and right ends of the tissue (Γ_D). The parameters used for the calculation are shown in Table I. The resulting value for the length constant is $\sigma = 0.71$ mm.

We perform the finite element calculations using the Matlab PDE toolbox. The implementation of the finite element method is based on the weak formulation of the mechanical bidomain model. The domain Γ is decomposed into a triangular mesh consisting of 800 two-dimensional plane elements (Fig. 7). On this mesh we define piecewise linear basis functions $\phi_i(x)$ for each node.

Table I. Parameter values used in the finite element calculation.

a	30 mm
L	5 mm
ν	10^4 Pa
μ	10^4 Pa
χ	10^8 Pa
δ	10^8 Pa
K	10^{10} Pa m^{-2}
F	1000 Pa

For our implementation, we chose $i = 1, 2, \ldots, N$, as hat functions that take the value 1 at the node i and 0 at all other nodes. These functions form a basis of dimension N of V_h, the space of continuous piecewise linear polynomials.

A plot of the intracellular vector displacement is shown in Figure 8. The extracellular displacement is nearly indistinguishable from the intracellular displacement when u_x and w_x are plotted together. The results are consistent with those predicted in Figure 4. Figure 9 shows a plot of u_x–w_x, and Figure 10 compares the analytical and numerical solutions in more detail. The membrane force is restricted to a thin boundary layer at the upper and lower tissue surfaces.

These results indicate that the numerical model, calculated using the finite element method, is consistent with the analytical solution derived in Section 3.1. Now that the model is verified using a known solution, we can apply it to new and more complex physical situations.

4. DISCUSSION

The two examples examined in this paper are simple enough to yield analytical solutions, but are complicated enough that they illustrate new features of the bidomain model that are not predicted by a monodomain model. Perhaps the most important prediction of the model is that, at least in this example, the membrane and therefore mechanotransduction is localized to the surface of the tissue, and falls off with distance from the surface by the length constant σ. This behavior was observed in other studies using the mechanical bidomain model, and appears to be a general result.[18,21] In this particular example, the shear strains given by (33)–(34) are *not* localized near the

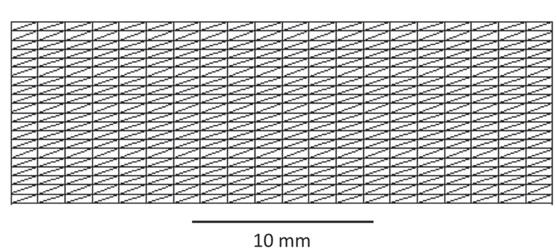

Fig. 7. The finite element mesh.

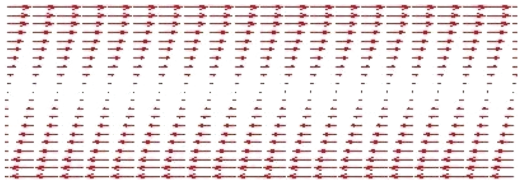

Fig. 8. The displacement **u**.

tissue surface. Therefore, the model makes a specific and testable prediction that may help determine if membrane forces (our hypothesis) or stress and strain (an alternative hypothesis) cause mechanotransduction.

The results of the mechanical bidomain model are consistent with both calculations and experiments based on a cell monolayer grown on an extracellular substrate. These experiments suggest that membrane or traction forces were restricted to a thin layer within a few tens of microns of the tissue edge.[29] The localization of the membrane forces to the edge was sensitive to intercellular cadherin-based adhesions,[28] which contribute to our intracellular moduli γ, ν, and χ. Experiments using cells having fewer intercellular connections should reduce the intracellualr shear modulus ν, thereby reducing the length constant σ.[28]

More complicated examples will require numerical methods to solve for the distribution of displacements and pressures. Previous finite element calculations based on a two-layer model (a contractile layer of cells and a passive layer of extracellular matrix) illustrate many of the features of our mathematical model.[29] In this paper, we present our first numerical solutions of the mechanical bidomain model based on the finite element method. The algorithm provides results that are consistent with known analytical solutions. The numerical method provides a path for modeling more complex biological problems.

The mechanical bidomain model has many limitations. It does not account for important features such as large deformations, plasticity, viscoelasticity, and fracture. The values of several of its paramenters are currently unknown, such as the membrane spring constant K and the relative contribution of the intracellular and extracellular spaces to the shear and bulk moduli, ν/μ and χ/δ. We have not yet incorporated fiber curvature into the intracellular stress tensor; currently we assume the fibers are all straight. Nevertheless, this model does highlight the role of membrane forces, a key feature that is not included in many other

Fig. 9. The difference $u_x - w_x$.

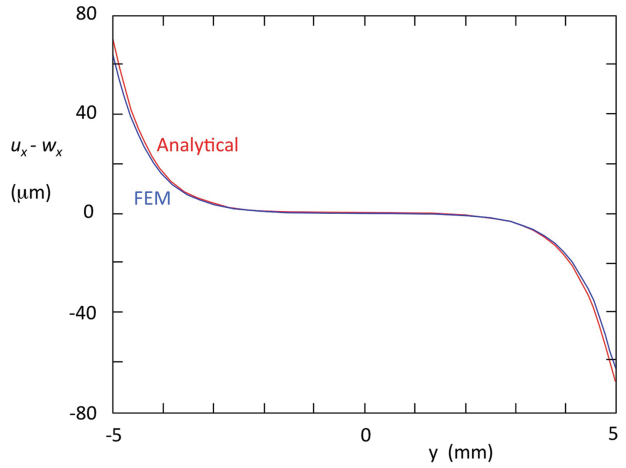

Fig. 10. A comparison of the analytical and numerical calculations along a line through the center for the tissue.

models. Future development of the model may incorprate many of these additional features to make the simulations more realistic.

One of the most interesting features of the model is its multiscale nature. The mechanical bidomain model is primarily a macroscopic model governing the mechanical displacements at the tissue or organ level. Our macroscopic formulation of the model has not yet been derived from a detailed representation of the cellular microstructure.[30, 31] A key development of the *electrical* bidomain model was its derivation from a cellular model.[32] Such a derivation for the *mechanical* bidomain model will provide additional insight into the interpretation of our macroscopic parameters such as the intracellular and extracellular moduli. On the other hand, the mechanical bidomain model connects the macroscopic length scale to the whole tissue and even whole organ scale. The model predicts new length scales, σ and ξ, that may be small compared to a whole organ. Elegant experiments[29] using cell monolayers suggest σ is on the order of tens of microns, but we do not know of similar data for intact tissue. We cannot calculate this length constant without knowing the value of the spring constant K. However, we do know that ξ is probably hundreds of times larger than σ,[23] so that they describe behavior over different length scales. Moreover, the model predicts membrane forces that are thought to act on individual proteins such as integrins. Thus, the model describes behavior from the organ level down to the molecular level, and is truly multiscale.

References and Notes

1. C. R. Jacobs, H. Huang, and R. Y. Kwon; Introduction to Cell Mechanics and Mechanobiology, Garland, New York **(2013)**.
2. F. Rodriguez, F. Langer, K. B. Harrington, A. Cheng, G. T. Daughters, J. C. Criscione, N. B. Ingels, and D. C. Miller; Cardiopulmonary support and physiology alterations in transmural strains adjacent to ischemic myocardium during acute midcircumflex occlusion; *J. Thorac. Cardiovasc. Surg.* 129, 791 **(2005)**.

3. P. H. M. Bovendeerd; Modeling of cardiac growth and remodeling of myofiber orientation; *J. Biomech.* 45, 872 **(2012)**.
4. M. Genet, L. C. Lee, R. Nguyen, H. Haraldsson, G. Acevedo-Bolton, Z. H. Zhang, L. Ge, K. Ordovas, S. Kozerke, and J. M. Guccione; Distribution of normal human left ventricular myofiber stress at end diastole and end systole: A target for in silico design of heart failure treatments; *J. Appl. Physiol.* 117, 142 **(2014)**.
5. R. Knoll, M. Hoshijima, H. M. Hoffman, V. Person, I. Lorenzen-Schmidt, M.-L. Bang, T. Hayashi, N. Shiga, H. Yasukawa, W. Schaper, W. McKenna, M. Yokoyama, N. J. Schork, J. H. Omens, A. D. McCulloch, A. Kimura, C. C. Gregorio, W. Poller, J. Schaper, H. P. Schultheiss, and K. R. Chien; The cardiac mechanical stretch sensor machinery involves a Z disc complex that is defective in a subset of human dilated cardiomyopathy; *Cell* 111, 943 **(2002)**.
6. W. Kroon, T. Delhass, P. Bovendeerd, and T. Arts; Computational analysis of the myocardial structure: Adaptation of cardiac myofiber orientations through deformation; *Med. Imag. Anal.* 13, 346 **(2009)**.
7. J. H. Omens; Stress and strain as regulators of myocardial growth; *Prog. Biophys. Mol. Biol.* 69, 559 **(1998)**.
8. A. W. Orr, B. P. Helmke, B. R. Blackman, and M. A. Schwartz; Mechanisms of mechanotransduction; *Developmental Cell* 10, 11 **(2006)**.
9. M. Chiquet; Regulation of extracellular matrix gene expression by mechanical stress; *Matrix Biology* 18, 417 **(1999)**.
10. M. Chiquet, L. Gelman, R. Lutz, and S. Maier; From mechanotransduction to extracellular matrix gene expression in fibroblasts; *Biochimica et Biophysica Acta* 1793, 911 **(2009)**.
11. B. E. Dabiri, H. Lee, and K. K. Parker; A potential role for integrin signaling in mechanoelectrical feedback; *Prog. Biophys. Mol. Biol.* 110, 196 **(2012)**.
12. C. Jean, P. Gravelle, J. J. Fournie, and G. Laurent; Influence of stress on extracellular matrix and integrin biology; *Oncogene* 30, 2697 **(2011)**.
13. A. Katsumi, A. W. Orr, E. Tzima, and M. A. Schwartz; Integrins in mechanotransduction; *J. Biol. Chem.* 279, 12001 **(2004)**.
14. E. A. Schwartz, R. Bizios, M. S. Medow, and M. E. Gerritsen; Exposure of human vascular endothelial cells to sustained hydrostatic pressure stimulates proliferation: Involvement of the alphaV integrins; *Circ. Res.* 84, 315 **(1999)**.
15. S. P. Gandhi and B. J. Roth; A numerical method of the mechanical bidomain model (submitted).
16. S. P. Gandhi, P. Lwin, and B. J. Roth; A numerical method to solve the mechanical bidomain model of cardiac tissue; *Michigan Academy of Science, Arts and Letters Conference*, Rochester, MI **(2014)**.
17. V. M. Punal and B. J. Roth; A perturbation solution of the mechanical bidomain model; *Biomechanics and Modeling in Mechanobiology* 11, 995 **(2012)**.
18. S. Puwal and B. J. Roth; Mechanical bidomain model of cardiac tissue; *Phys. Rev. E* 82, 041904 **(2010)**.
19. S. Puwal; Two-domain mechanics of a spherical, single chamber heart with applications to specific cardiac pathologies; *SpringerPlus* 2, 187 **(2013)**.
20. B. J. Roth; The mechanical bidomain model: A review; *ISRN Tissue Engineering* 2013, 863689 **(2013)**.
21. B. J. Roth; Boundary layers and the distribution of membrane forces predicted by the mechanical bidomain model; *Mechanics Research Communications* 50, 12 **(2013)**.
22. B. J. Roth; Using the mechanical bidomain model to analyze the biomechanical behavior of cardiomyocytes; *Methods in Molecular Biology* 1299, 93 **(2015)**.
23. K. Sharma and B. J. Roth; How compressibility influences the mechanical bidomain model; *Biomath* 3, 1411171 **(2014)**.
24. E. L. Barker, R. T. Bonnecaze, and M. H. Zaman; Extracellular matrix stiffness and architecture govern intracellular rheology in cancer; *Biophys. J.* 97, 1013 **(2009)**.
25. V. Gupta and K. J. Grande-Allen; Effects of static and cyclic loading in regulating extracellular matrix synthesis by cardiovascular cells; *Cardiovasc. Res.* 72, 375 **(2006)**.
26. J. Y. Kresh and A. Chopra; Intercellular and extracellular mechanotransduction in cardiac myocytes; *Pflugers Archiv European J. Phys.* 462, 75 **(2011)**.
27. S. R. Peyton, C. M. Ghajar, C. B. Khatiwala, and A. J. Putnam; The emergence of ECM mechanics and cytoskeletal tension as important regulators of cell function; *Cell Biochem. Biophys.* 47, 300 **(2007)**.
28. A. F. Mertz, Y. Che, S. Banerjee, J. M. Goldstein, K. A. Rosowsk, S. F. Revilla, C. M. Niessen, M. C. Marchetti, E. R. Dufresne, and V. Horsley; Cadherin-based intercellular adhesions organize epithelial cell-matrix traction forces; *Proc. Natl. Acad. Sci.* 110, 842 **(2013)**.
29. C. M. Nelson, R. P. Jean, J. L. Tan, W. F. Liu, N. J. Sniadecki, A. A. Spector, and C. S. Chen; Emergent patterns of growth controlled by multicellular form and mechanics; *Proc. Natl. Acad. Sci.* 102, 11594 **(2005)**.
30. Z. Chen, S. Jiang, Y. Gan, H. Liu, and T. D. Swell; A particle-based multiscale simulation procedure within the material point method framework; *Computational Particle Mechanics* 1, 147 **(2014)**.
31. H. Lu, N. Daphalapurkar, B. Wang, S. Roy, and R. Komanduri; Multiscale simulation from atomistic to continuum-coupling molecular dynamics (MD) with the material point method (MPM); *Philosophical Magazine* 86, 2971 **(2006)**.
32. J. C. Neu and W. Krassowska; Homogenization of syncytial tissues; *Crit. Rev. Biomed. Eng.* 21, 137 **(1993)**.